The Scaling Effect of Graphene-Based Hybrid Photodetectors

The Scaling Effect of Graphene-Based Hybrid Photodetectors

Qiming Wu[1, 2, a], Jun Shen[1, 2, b], and Huabin Wang[1, 2, *]

[1]Chongqing Institute of Green and Intelligent Technology, Chinese Academy of Sciences, Chongqing, China;
[2]University of Chinese Academy of Sciences, Beijing, China.

*Corresponding author e-mail: wanghuabin@cigit.ac.cn, [a]2318524856@qq.com, [b]shenjun@cigit.ac.cn

Abstract. Graphene-based hybrid photo detectors are promising for weak-light detection with high photo gain. In this paper, we focused on the details of the scaling effect on grapheme-based hybrid photo detectors. By designing a series of devices with different sizes from 10*10μm^2 to 100*100μm^2, we found that the photocurrent generally decreases with increased channel length but decreased channel width. Our study would be useful for clarifying the real potential of photo gating effect in image applications.

1. Introduction

Graphene is thought to be a promising material for novel photodetectors due to its high carrier mobility and broadband photo response [1-3]. However, monolayer grapheme can absorb only 2.3% of the incident light, making its application in photodetectors limited. By combining grapheme with colloidal-quantum-dot (CQD), Gerasimos Konstantatos et al. designed grapheme–quantum dot phototransistors in 2012, taking advantage of high light absorption of quantum dots and high carrier mobility of grapheme, reaching a responsively of ~10^{7}A/W [4]. The principal mechanism supporting this ultrahigh responsively is the photo gating effect, which make use of the field effect to induce high gain. Based on this effect, in 2016, Ivan Nikiski et al. made a transparent indium tin oxide (ITO) top-contact electrode to CQD-grapheme hybrid photo detector, and the device realized quantum efficiencies excess of 70% [5], while Golam Haider et al. designed composite grapheme-quantum dot hybrid photo detector on lead zircon ate titanate (PZT) substrates which could get ultrahigh responsively as 4.06*10^{9}A/W under 325 nm UV light illumination [6]. In 2017, Stijn Goossens et al. reported the realization of an image sensor of grapheme–quantum dot photo detectors as a digital camera with high sensitivity for both visible and shortwave infrared light [7]. In this paper, we discussed the scaling effect of grapheme-based hybrid photo detectors using grapheme-silicon heterojunction structure [8, 9] with photo gating effect under visible light illumination. Our experiments demonstrated the scaling effect of grapheme hybrid photo detectors, and our results could be further extended to other structures or materials, such as devices with hybrid quantum dots, nanowires or perovskite [10, 11, and 12].

2. Experiments

Graphene film used for our experiments was synthesized by chemical vapor deposition (CVD) [13, 14] on Cu. Subsequently the grapheme was transferred to intrinsic silicon substrates by wetting transfer

method with 4% hydrochloric acid (HCl) and 10% hydrogen peroxide (H_2O_2), as well as 4% poly methyl methacrylatemethacrylic acid (PMMA). The electrode patterns were fabricated by double-layer photoresist technology with LOR photoresist depositing by spin coater as the first layer, and then S1805 photoresist as the second layer. The aim of double layer photoresist was to take advantage of the inverted trapezoidal structure to lift off metals bitterly. Then the patterns were exposed by mobile mask exposure machine with ultraviolet light in 27s following developing in 50s. The metal electrode patterns were made with chromium (3nm) deposited at room temperature by electron beam evaporation then gold (100nm) by thermal evaporation at pressure of $5*10^{-4}$ Pa followed by a lift-off process in warm acetone. And then use similar progresses of previous exposure to make grapheme strips between the Au electrodes. The channel lengths of strips vary from 100μm to 10μm as well as the channel width varies. Following by ion bean etcher to etch the grapheme flakes to desired dimensions, use 400K developing solution and warm acetone to wipe off the double-layer photoresist, S1805 and LOR.

Electrical measurements were performed under voltage bias on the electrodes at room temperature in air using a Keithely 4200 instrumentation with laser beam of 635nm. The samples were characterized by scanning electron microscope (SEM) to determine the surface coverage and then by Raman to define the components in sample. Also, we used Xenon lamp spectrometer to measure the spectral response of samples in visible range as well as a Keithely 7510 instrumentation to test the rapid response of the devices.

3. Results and discussion

The structure of grapheme–silicon heterostructure photo detector are shown in Figure 1(a) and 1(b). The start wafer we employed is intrinsic silicon. Then, the CVD grown grapheme is transferred, and metal electrodes are deposited on grapheme. Use exposure, developing and etching progresses to make the patterns we want and get rid of needless grapheme. Apparently when the intrinsic silicon and grapheme contracts, there will be a band bending from grapheme to intrinsic silicon, leading electrons transiting into intrinsic silicon then forms a built-in field at the surface. As the visible light illuminates in, pairs of carries separate and under the built-in field effect, electrons transit in grapheme forming photocurrent in the device. Figure 1(b) shows the actual structure after processes by scanning electron microscope (SEM), we can see the electrodes and grapheme strip clearly. The size of the strip is $80*40\mu m^2$.

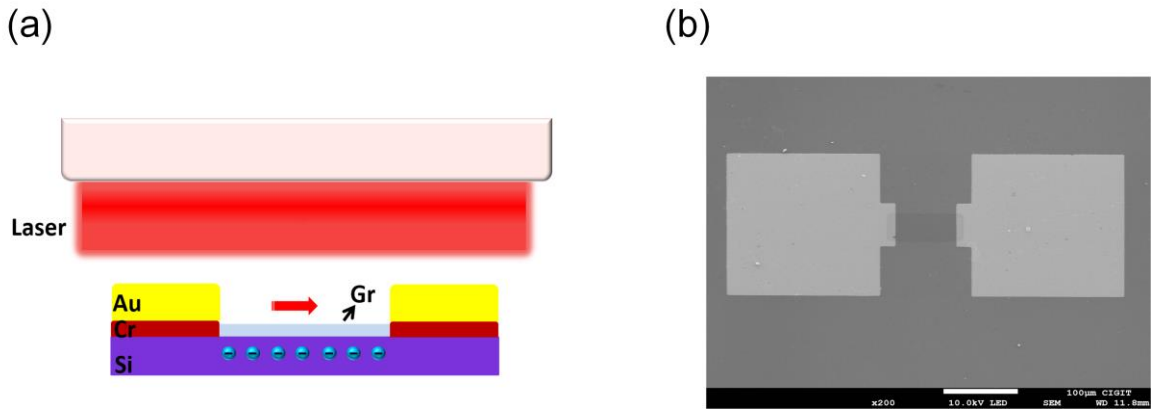

Figure 1. (a) The model and schematic of the device. The heterojunction of the grapheme-silicon generates photo gating effect at the surface when visible light illuminates, the photo induced electrons transits in the grapheme between the electrodes producing photocurrent. (b) The actual structure photo of SEM.

To explore the influence of device size on photo detector response, we designed a series of devices with channel length and width ranging from 10um to 100um and tested their parameters under 635nm laser beam illuminating of uniformly 20μW laser output power. Figure 2(a) shows the photocurrent and responsively as a function of channel length for given channel width between the grapheme and the gold, while in Figure 2(b) on the contrary taken channel width as variety. As shown in Figure 2(a), for given channel width, the photocurrent generally decreases with the increasing channel length. It suggests that with channel length increasing, it takes more time for electrons to transit inside grapheme meantime the resistance increases, both these factors result into this decrease. However, in Figure 2(b) for given channel length the photocurrent obviously increases as the channel width increasing. Though the resistance of the structure increases, wider contract may proceed more ways for carriers (most are electrons) to transit, which takes more essential part than the resistance. And under the action of the same laser output power of 20μW, the variation trend of the responsively is the same as that of the photocurrent.

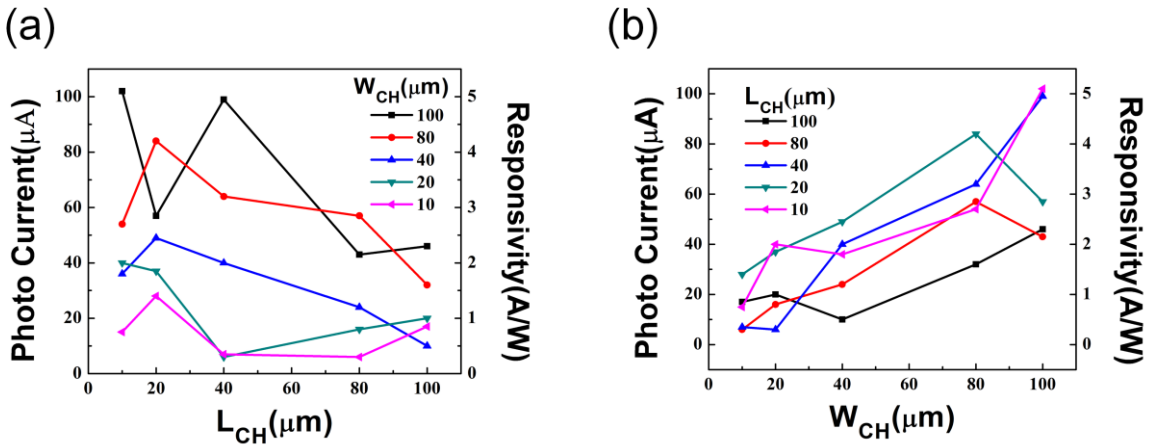

Figure 2. (a) The photocurrent and responsively as a function of channel length under 635nm laser beam illuminating of uniformly 20μW laser output power by Keithely 4200. (b) The channel width dependence at the same experiment condition as (a).

However, due to the differences in channel lengths or channel widths, properties of devices are affected by the differences in resistance of scaling. To exclude its distraction, we desire to compare devices which in different sizes but have the same proportion with channel length and channel width in 1:1 (For eg.80 *80μm^2) and explore their differences. Figure 3(a) and 3(b) are the relationship of responsively and specific detectivity with channel length under laser output power in the logarithmic form. For responsively, several groups of devices show similar curves. The responsively increases with the increase of device size and the decrease of power. For specific detectivity, curves also show good linearity taking the logarithm for device size, the specific detectivity increases with increasing device size and decreasing laser output power.

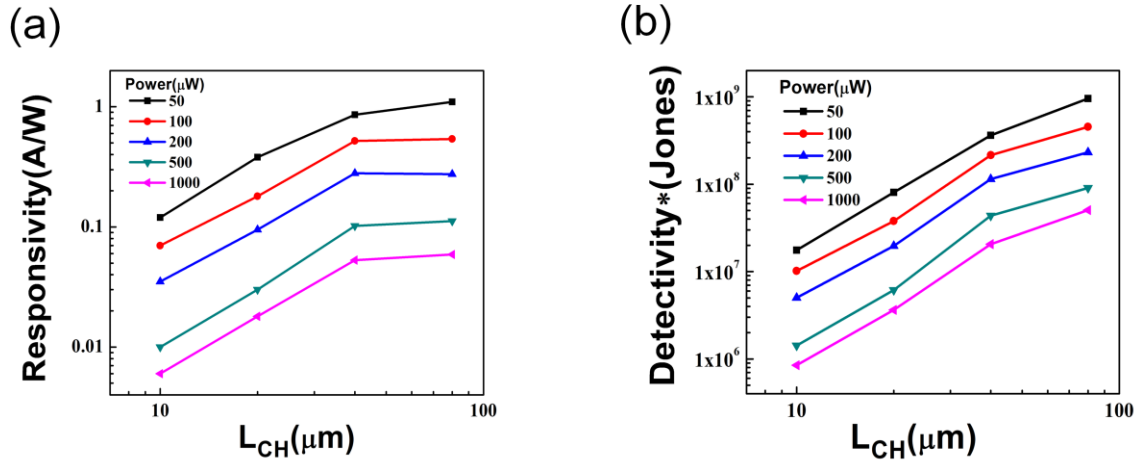

Figure 3. (a) Comparison with laser output powers, for scaling effect of devices with the same channel length/width ratio of 1:1of responsivity taking the logarithm of the two axes respectively, and (b) is the result of specific detectivity.

Figure 4(a) shows the rapid response of 100*100μm^2 device with a period of 10ms with both rising edge time and falling edge time for about 200μs. Figure 4(b) shows the spectral response of devices under visible lights from 500nm to 750nm by Xenon lamp spectrometer. We choose three sizes (still 1:1 length/width ratio), 80μm, 20μm and 10μm to compare their differences. The response of 10μm and 20μm are apparently higher than 80μm, indicating though small devices show lower current cause of their size, their responsivity are really high for effectively making use of light power. The maximum responsivity is about 7014 A/W for 10μm device at 500nm illuminating indicating the advantage of photogating effect of graphene-silicon structure.

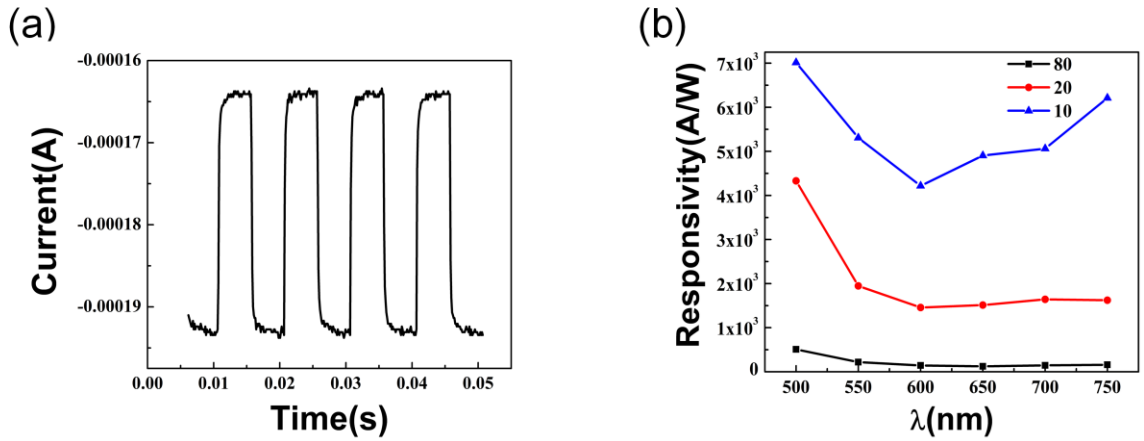

Figure 4. (a) Comparison with laser output powers, for scaling effect of devices with the same channel length/width ratio of 1:1of responsively taking the logarithm of the two axes respectively, and (b) is the result of specific detectivity.

4. Conclusion

In conclusion, we explored the influence of device size and incident power on grapheme hybrid photo detectors adopting photo gating effect. Generally, the photocurrent increases as decreasing the channel length and increasing the channel width. After excluding the influence of resistance, with devices in same ratio of 1:1, the responsively increases with the size of the devices, while larger device sizes and

smaller power are preferred for larger specific detectivity. For rapid response, our devices show about 200μs both for rising edge time and falling edge time. As for spectral response of the devices, small devices show higher responsively for about 7014A/W in peak due to the high-effective use for light power.

Acknowledgments
This work was supported by NSFC (No. 61705229), and the Fundamental and Advanced Research Project (Key Program) of Chong Qing Municipality (cstc2015jcyjBX0046).

References
[1] Koppens F H L, Mueller T, Avouris P, et al. Photodetectors based on graphene, other two-dimensional materials and hybrid systems [J]. Nature Nanotechnology, 2014, 9(10):780-793.
[2] Avouris P, Freitag M. Graphene Photonics, Plasmonics, and Optoelectronics [J]. IEEE Journal of Selected Topics in Quantum Electronics, 2013, 20(1):72-83.
[3] Bonaccorso F, Sun Z, Hasan T, et al. Graphene Photonics and Optoelectronics [J]. Nature Photonics, 2010, 4(9):611-622.
[4] Konstantatos G, Badioli M, Gaudreau L, et al. Hybrid graphene–quantum dot phototransistors with ultrahigh gain [J]. NATURE NANOTECHNOLOGY, 2012, 7(6):363-368.
[5] Nikitskiy I, Goossens S, Kufer D, et al. Integrating an electrically active colloidal quantum dot photodiode with a graphene phototransistor [J]. Nature Communications, 2016, 7:11954.
[6] Haider G, Roy P, Chiang C-W, et al. Electrical-Polarization-Induced Ultrahigh Responsivity Photodetectors Based on Graphene and Graphene Quantum Dots [J]. Advanced Functional Materials, 2016, 26(4):620-628.
[7] Goossens S, Navickaite G, Monasterio C, et al. Broadband image sensor array based on graphene–CMOS integration [J]. Nature Photonics, 2017, 11(6):366-371.
[8] Kumar R, Varandani D, Mehta B R. Nanoscale interface formation and charge transfer in graphene/silicon Schottky junctions; KPFM and CAFM studies [J]. Carbon, 2015, 98:41-49.
[9] An X, Liu F, Kar S. Optimizing performance parameters of graphene–silicon and thin transparent graphite–silicon heterojunction solar cells [J]. Carbon, 2013, 57:329-337.
[10] Kind H, Yan H Q, Messer B, et al. Nanowire Ultraviolet Photodetectors and Optical Switches [J]. Advanced Materials, 2002, 14(2):158-160.
[11] Sun Z, Liu Z, Li J, et al. Infrared Photodetectors Based on CVD-Grown Graphene and PbS Quantum Dots with Ultrahigh Responsivity [J]. Advanced Materials, 2012, 24(43):5878-5883.
[12] Lee Y, Kwon J, Hwang E, et al. High-Performance Perovskite-Graphene Hybrid Photodetector [J]. Advanced Materials, 2015, 27(1):41-46.
[13] Suk J W, Kitt A, Magnuson C W, et al. Transfer of CVD-grown monolayer graphene onto arbitrary substrates.[J]. Acs Nano, 2011, 5(9):6916-6924.
[14] Li X, Cai W, An J, et al. Large-Area Synthesis of High-Quality and Uniform Graphene Films on Copper Foils [J]. Science, 2009, 324(5932):1312-1314.